Encapsulation of TiO_2 nanoparticles into single-walled carbon nanotubes

2009 New J. Phys. 11 093011

(http://iopscience.iop.org/1367-2630/11/9/093011)

New Journal of Physics
The open-access journal for physics

Encapsulation of TiO_2 nanoparticles into single-walled carbon nanotubes

Duangkamon Baowan[1], Wannapong Triampo[2,3,5] and Darapond Triampo[4]

[1] Department of Mathematics, Faculty of Science, Mahidol University, Rama VI, Bangkok 10400 Thailand; Centre of Excellence in Mathematics, CHE, Si Ayutthaya Road, Bangkok 10400, Thailand
[2] R&D Group of Biological and Environmental Physics (BIOPHYSICS), Department of Physics, Faculty of Science, Mahidol University, Bangkok 10400 Thailand; ThEP Center, CHE, 328 Si Ayutthaya Road, Bangkok 10400, Thailand
[3] Center for Vectors and Vector-Borne Diseases, Mahidol University, Nakhonpathom 73170, Thailand
[4] Chemistry Department, Center of Excellence for Innovation in Chemistry, Faculty of Science, Mahidol University, Rama VI, Bangkok 10400, Thailand
E-mail: scwtr@mahidol.ac.th

New Journal of Physics **11** (2009) 093011 (13pp)
Received 13 May 2009
Published 14 September 2009
Online at http://www.njp.org/
doi:10.1088/1367-2630/11/9/093011

Abstract. Nanostructures such as carbon nanotubes and titanium dioxide (TiO_2) offer the means to create novel nanoscale devices and technologies. The question as to whether or not TiO_2-nanoparticle (TiO_2-NP) can be encapsulated in a single-walled carbon nanotube (SWNT) depends on the physical and chemical interactions between the TiO_2-NP and the SWNT. Motivated by nanoscale encapsulation research and nanoscale delivery systems, we present a simple but useful model to study the system comprised of an SWNT encapsulated with TiO_2-NP under various conditions. Using the well-known Lennard-Jones (6–12) potential for both cylindrical- and spherical-shaped TiO_2-NP, analytical expressions are obtained for calculating the potential energy, the encapsulating energy and the force distribution and other quantities. In particular, the suction force experienced by an SWNT located near an open end of a

[5] Author to whom any correspondence should be addressed.

semi-infinite SWNT is considered. It is found that the calculated condition for the suction behavior depends only on the difference of their radii ($b - a$): cylindrical TiO_2-NP $b - a = 3.561$ Å and spherical TiO_2-NP $b - a = 3.304$ Å. Connection with a possible drug delivery application is also discussed.

Contents

1. Introduction

Carbon nanotubes (CNTs) constitute perhaps the most well-known nanoparticle studied so far. Single-walled carbon nanotubes (SWNTs) are by far the most promising material for nanodevices because of their unusual and unique physical, chemical and electronic properties [1, 2]. Hence, SWNTs can provide a unique opportunity for the nanoscale engineering of novel one-dimensional systems, created by the self-assembly of molecules inside the SWNT's hollow core. Materials confined in such small cavities are expected to show novel features that are not observed in bulk materials [3]–[5]. Among this class of materials, SWNT filled with fullerenes (e.g. C_{60}), the so-called 'peapods', have attracted considerable attention. It has been experimentally shown that fullerenes can be inserted into SWNTs, forming a peapod-like structure [6]–[10]. The composite nature of peapod-like materials raises the exciting possibility of a nanoscale material that can be designed for a particular electronic and mechanic functionality. However, the formation mechanisms of nanopeapods are currently unknown. Regarding the unique properties underlie distinguishable from microscale or bulk systems, this involves the van der Waals interaction force and the large surface to volume ratio of nanoparticles.

Titanium dioxide (TiO_2), sometimes referred to as titania, has attracted attention as an alternative material for a number of applications including water and air purification, photocatalytic sterilization in food and the environmental industry [11, 12]. It has been intensively used on a wide spectrum of organisms including bacteria [13], fungi, algae, viruses [14, 15] and cancer cells [16, 17]. When TiO_2 absorbs ultraviolet A (UV-A) light with a wavelength less than 385 nm or an energy greater than the band gap of TiO_2, it generates electron–hole pairs and migrates to the surface through diffusion and drift [18], in competition with a multitude of trapping and recombination events in the lattice bulk. On the photocatalyst surface, TiO_2 particles yield superoxide radicals ($O_2^{\bullet -}$) and hydroxyl radicals (•OH) that can initiate oxidants [19]. The hydroxyl radicals are particularly highly active for both the oxidation of organic substances and the inactivation of bacteria and viruses [20]. Most studies conclude that •OH is the main cause of the bactericidal effect of photocatalysis [21, 22], but the actual basis for this effect is not well understood. Furthermore, the surface properties of TiO_2 are well

known because this solid has been widely investigated by a variety of physicochemical methods. Once again, although the experimental knowledge is extensive, the process fundamentals are yet to be fully understood. In addition, the relatively low cost, ease of location, non-toxic (dose dependent), stable and high oxidative power characteristics, make this material ideal for characterization and photocatalytic studies. The only serious drawback of TiO_2 is that its band gap lies in the near-UV of the electromagnetic spectrum: 3.2 eV (285 nm) and 3.0 eV (410 nm) for the two forms anatase and rutile, respectively.

CNT-based hybrid materials in combination with TiO_2 have many potential important applications. To the best of our knowledge, our study is the first time the feasibility and optimality of encapsulation of TiO_2 nanoparticle in SWNT have been investigated. In this paper, we present a simple but useful model based on straight forward algebraic calculation using the Lennard-Jones (6–12) potential as the force field. Concerning both cylindrical and spherical shape TiO_2 particles, analytical expressions for calculating the potential energy, encapsulating energy and force distribution and the consequent predicted results are obtained. We anticipate that this model will allow us to utilize these two particles in many novel nanoscaled applications. We also believe that this work could impact therapeutic research, especially drug delivery systems based on nanodevices. The paper is organized as follows. The potential function of the TiO_2-SWNT system is described in the next section. In sections 3 and 4, the results, including analytical and numerical results for the cylindrical and spherical TiO_2 encapsulation, are presented. Section 5 presents some implications of our predictions for certain applications, and we make some concluding remarks.

2. Potential energy, encapsulation energy and force distribution

The interaction energy between a CNT and TiO_2 is investigated using the Lennard-Jones potential function [23]. We assume that all the carbon atoms on the CNT are uniformly distributed, so that we may utilize the continuum approximation. We note that the continuum approach has been successfully used in many applications to determine the interaction energy between two carbon nanostructures [24]–[33]. For TiO_2, the anatase structure, as shown in figure 1, is considered because it occurs most frequently in the experiments [34]. Anatase is one of the three mineral forms of TiO_2, the other two being brookite and rutile, and it has a tetragonal crystal structure with $a = b = 3.784$ Å and $c = 9.515$ Å [34].

The classical Lennard-Jones potential for two atoms is given by

$$\Phi = -\frac{A}{\rho^6} + \frac{B}{\rho^{12}}, \tag{1}$$

where ρ denotes the distance between the two surface elements and A and B are the attractive and repulsive constants, respectively. Equation (1) can also be written in the form

$$\Phi = 4\epsilon \left[-\left(\frac{\sigma}{\rho}\right)^6 + \left(\frac{\sigma}{\rho}\right)^{12} \right],$$

where σ is the van der Waals diameter. The equilibrium distance ρ_0 is given by $\rho_0 = 2^{1/6}\sigma$ and the well depth $\epsilon = A^2/(4B)$. When information is lacking, it is possible to use the empirical combining laws or mixing rules [35], thus $\epsilon_{12} = (\epsilon_1\epsilon_2)^{1/2}$ and $\sigma_{12} = (\sigma_1 + \sigma_2)/2$, where 1 and 2 refer to the respective individual atoms.

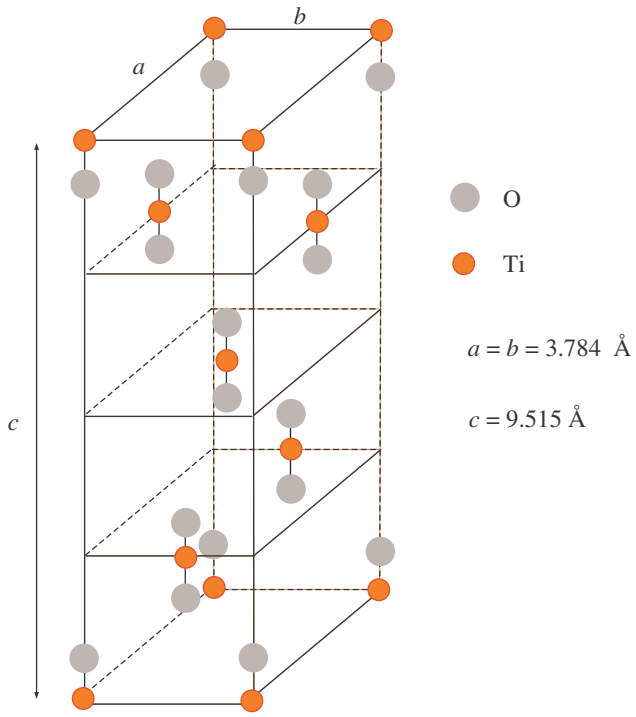

Figure 1. Anatase structure of TiO_2.

By utilizing the continuum approach, the interaction energy between two molecules can be obtained by performing double surface integrals, averaged over the surfaces of each entity

$$U = \eta_1 \eta_2 \int \int \Phi(\rho)\, \mathrm{d}S_1\, \mathrm{d}S_2,$$

where η_1 and η_2 are the mean atomic surface density of atoms on each molecule and, again, ρ denotes the distance between two typical surface elements $\mathrm{d}S_1$ and $\mathrm{d}S_2$ on each molecule.

The resultant axial force (z-direction) is obtained by differentiating the integrated Lennard-Jones potential with respect to Z, which is the distance in the axial direction of the tube, so that the force can be written as

$$F_Z = -\frac{\partial U}{\partial Z}. \tag{2}$$

Here, our aim is to determine the nanotube radius that gives the maximum suction force exerted on the TiO_2 molecule. The definition of *suction energy* was first described by Cox *et al* [24] and is defined as the total energy or work done generated by van der Waals interactions acquired by a particular molecule as a consequence of being sucked into the nanotube, namely

$$W = \int_{-\infty}^{\infty} F(Z)\, \mathrm{d}Z = -\int_{-\infty}^{\infty} \frac{\mathrm{d}U}{\mathrm{d}Z} \mathrm{d}Z = U(-\infty) - U(\infty),$$

which is the work done that is transformed into kinetic energy.

In this paper, we assume two geometric shapes for TiO_2: cylindrical and spherical, as shown in figure 2. An excellent review concerning TiO_2 and it synthesis is given in [34].

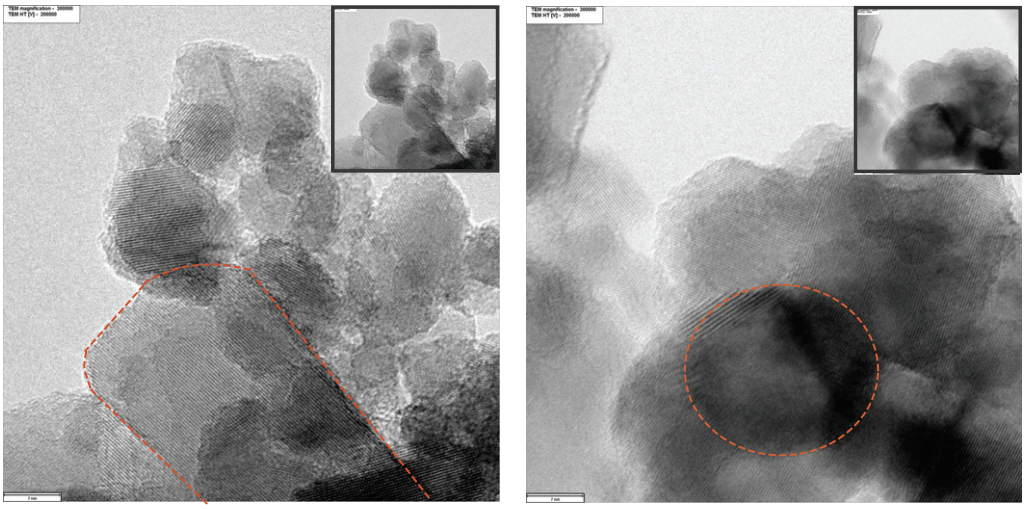

(a) Cylindrical shape (b) Spherical shape

Figure 2. The cylindrical shape (a) and the spherical shape (b) of TiO_2 occurring in our experiments.

3. Cylindrical geometry for TiO_2

In this section, we assume that the TiO_2 molecule can be modeled as a cylindrical shape. Firstly, the energy and the force distribution between the TiO_2 and the CNT are investigated. It can be shown that for a certain radius of CNT, the TiO_2 molecule will remain inside the tube. On the other hand, such molecules will not be encapsulated into the CNT if the tube radius is too small. Next, we wish to find the optimum radius of the CNT that gives the maximum interaction energy, which can be determined utilizing the suction energy.

The interaction between the TiO_2 and the CNT in the continuum approximation is obtained by averaging the atoms over the surfaces of each of the two molecules. With reference to a rectangular Cartesian coordinate system (x_1, y_1, z_1) with origin located at the center of the TiO_2 molecule, a typical point on the surface of the TiO_2 has coordinates $(a\cos\theta_1, a\sin\theta_1, z_1)$, where a is assumed to be the radius of the cylindrical TiO_2 of length $2L_1$. Similarly, with reference to a rectangular Cartesian coordinate system (x_2, y_2, z_2) with the origin located at the center of the CNT, a typical point on the surface of the tube has coordinates $(b\cos\theta_2, b\sin\theta_2, z_2)$, where b is the radius of the CNT assumed to be of length $2L_2$, as shown in figure 3. Note that this approach has been previously used in [33] to determine the energy and the force distribution for double-walled CNTs.

Now, we introduce a parameter Z, which is the distance between the centers that can be either positive (inside the tube) or negative (outside the tube); and the distance ρ between two typical points is given by

$$\begin{aligned}\rho^2 &= (b\cos\theta_2 - a\cos\theta_1)^2 + (b\sin\theta_2 - a\sin\theta_1)^2 + (z_2 - z_1)^2 \\ &= a^2 + b^2 - 2ab\cos(\theta_1 - \theta_2) + (z_2 - z_1)^2.\end{aligned}$$

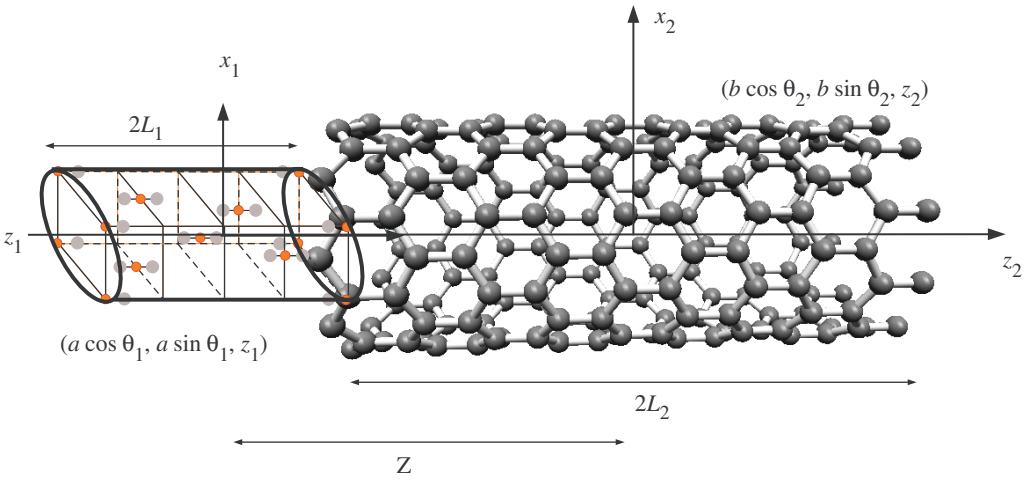

Figure 3. Energy and force distribution for cylindrical TiO_2 entering a symmetrically CNT.

Table 1. Lennard-Jones constants for the C–TiO_2 system (* [37]).

Interaction	ϵ (meV)	σ (Å)	A (eV × Å^6)	B (eV × Å^{12})
C–Ti	3.14	3.7588	35.38	99795.40
C–O	4.14	3.2531	19.61	23241.81
Graphene–graphene	3.83*	2.39*	15.2*	24100*

From the Lennard-Jones potential, the total energy of the system is given by

$$U = ab\eta_1\eta_2 \int_0^{2\pi}\int_0^{2\pi}\int_{-L_2}^{L_2}\int_{Z-L_1}^{Z+L_1}\left(-\frac{A}{\rho^6}+\frac{B}{\rho^{12}}\right)\mathrm{d}z_1\,\mathrm{d}z_2\,\mathrm{d}\theta_1\,\mathrm{d}\theta_2, \tag{3}$$

where η_1 and η_2 denote the mean atomic surface density of TiO_2 and CNT, respectively; and we note that the force distribution can be determined using the relation in (2). The suction energy is the total work performed on the two molecules, and since the van der Waals force is a short range interaction, the CNT is assumed to be semi-infinite in length. On using the continuum approximation and the Lennard-Jones potential function, the suction energy is given by

$$U = ab\eta_1\eta_2 \int_0^{2\pi}\int_0^{2\pi}\int_0^{\infty}\int_{Z-L_1}^{Z+L_1}\left(-\frac{A}{\rho^6}+\frac{B}{\rho^{12}}\right)\mathrm{d}z_1\,\mathrm{d}z_2\,\mathrm{d}\theta_1\,\mathrm{d}\theta_2, \tag{4}$$

where in this case, Z denotes the distance between the center of TiO_2 and the tube's open end.

Specifically, there are two different interactions for the interaction energy between TiO_2 and a CNT which are C–Ti and C–O, so that the total energy can be obtained as

$$U^{\mathrm{Tot}} = \frac{\eta_1}{3}\eta_2 U^*(A_{\mathrm{C-Ti}}, B_{\mathrm{C-Ti}}) + \frac{2\eta_1}{3}\eta_2 U^*(A_{\mathrm{C-O}}, B_{\mathrm{C-O}}), \tag{5}$$

where $U^*(A, B)$ is defined by $U^* = U/(\eta_1\eta_2)$ and U is given by (4). The Lennard-Jones constants A and B for the C–TiO_2 system are given in table 1, where the constants for C, Ti and O are taken from the work of Mayo *et al* [36].

The mean atomic surface density of TiO_2 η_1 is calculated from a single unit cell of the anatase structure, which consists of two TiO_2 units, and we may deduce $\eta_1 = 0.07498\,\text{Å}^{-2}$. In the case of η_2, we simply utilize the mean atomic surface density of a graphene sheet. This is because a CNT can be thought of as a graphene sheet rolled up to form a cylinder, and thus we may have $\eta_2 = 0.3812\,\text{Å}^{-2}$.

Assuming that the TiO_2 molecule is symmetrically located as indicated in figure 3 and is initiated from rest outside the CNT in the negative z-direction, the interaction energy and the force distribution are as shown in figure 4. In terms of the energy, as illustrated in figure 4(b), we fix the radius of TiO_2 to be $b = 2.6757$ Å, and we give two examples of CNTs of radii $b = 5.5757$ and 6.1757 Å. The cylindrical TiO_2 will be encapsulated into the tube if the potential energy inside the tube is less than that outside of it. It is clearly seen from figure 4(b) that when $b = 5.5757$ Å, the energy outside the tube is much lower than that inside, and therefore the TiO_2 molecule will not be encapsulated into this CNT. On the other hand for $b = 6.1757$ Å, the TiO_2 molecule will be encapsulated into the CNT since the potential energy inside the tube is lower than that outside of it.

Figure 4(c) shows the force distribution profiles for the two systems described above. We observe the step function arising at both of the tubes' open ends. As mentioned the TiO_2 is assumed to be initiated from rest outside the tube in the negative direction, so that the TiO_2 will move in the positive direction into the tube. In order for the TiO_2 to be encapsulated into the tube, the force on the negative side of the tube open end has to be positive to attract the TiO_2 in, and the force on the positive side of the tube open end has to be negative to repulse the TiO_2 molecule back and not let it escape. From figure 4, we see that this phenomenon occurs for $b = 6.1757$ Å but not for $b = 5.5757$ Å.

Furthermore, we aim to determine the radius of CNT for which the cylindrical TiO_2 can be encapsulated. Figure 5 shows an example of the suction profile for a unit cell of anatase TiO_2, $a = 2.6757$ Å, for various CNTs. The TiO_2 will be encapsulated into the CNT if the suction energy is positive. From the graph, we can see that the suction energy is zero when $b = b_0 = 5.6943$ Å, which is the point at which the TiO_2 begins to enter into the tube. As determined in the previous section, the encapsulation process occurs when $b > b_0$. The maximum suction energy occurs when the nanotube radius is $b = 6.2362$ Å, which gives rise to $b - a = 3.561$ Å. The maximum suction energy is insensitive to the change of their radii, where we find that $a - b$ is approximately 3.5605 Å to achieve such a maximum value. However, the change of TiO_2 length has an effect on the third and fourth decimal places of this value. Note that three TiO_2 radii, which are $a = 2.6757$, 4 and 6 Å, are examined for this work. Moreover, we find that the maximum suction energy is linearly dependent on the TiO_2 radius, wherein we may deduce

$$\text{Maximum suction energy (eV)} = 0.54a(\text{Å}) + 0.91.$$

4. Spherical geometry for TiO_2

In this section, the TiO_2 molecule is assumed to be a sphere. Again, we first examine the energy and the force distribution for a TiO_2 molecule inside a CNT in order to determine whether or not the TiO_2 molecule will remain inside the tube. After that, the suction energy is utilized to find the optimum value of the nanotube radius that gives the maximum interaction energy. The interaction energy and the force distribution for a spherical TiO_2 and a CNT, as shown in figure 6, are now determined. With reference to a rectangular Cartesian coordinate system

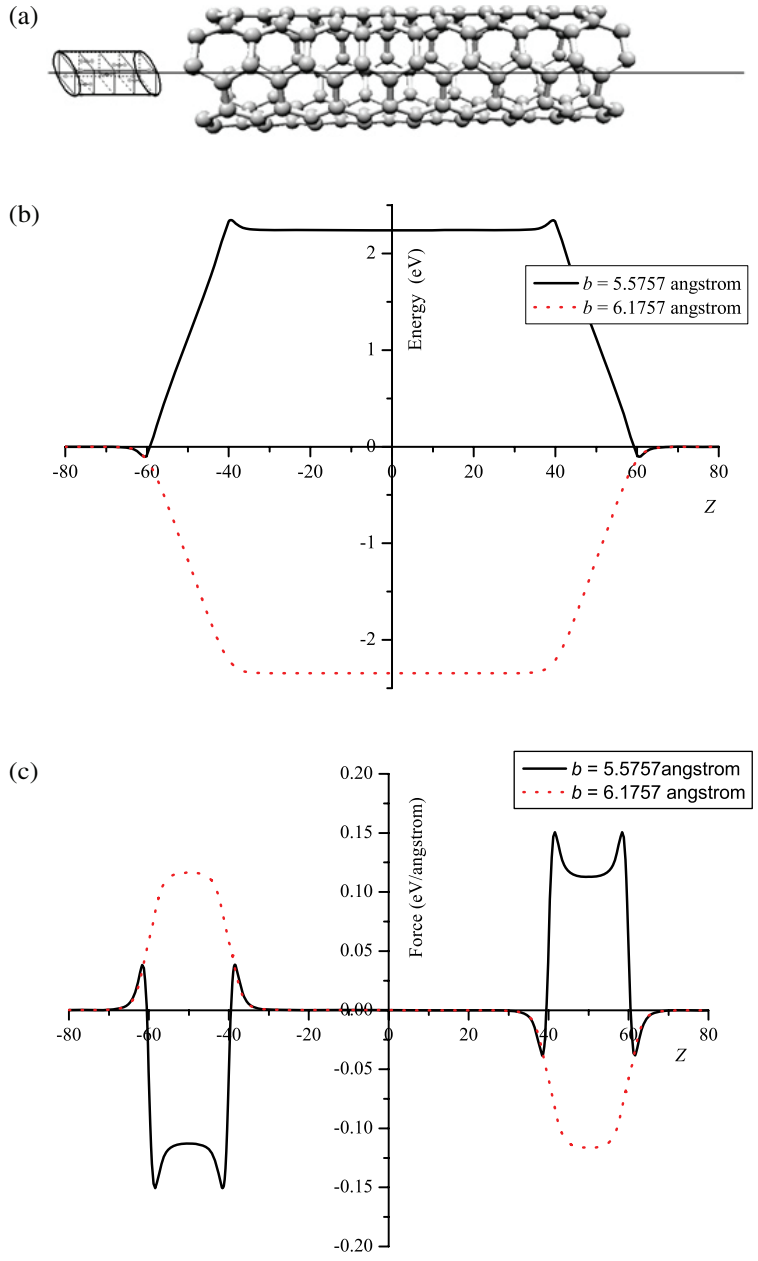

Figure 4. Cylindrical TiO_2 (a) with energy profile (b) and force distribution (c), where $a = 2.6757$ Å, $b = 5.5757$ and 6.1757 Å, $L_1 = 10$ Å and $L_2 = 50$ Å.

(x, y, z) with its origin located at the tube center, a typical point of the surface of the tube has the coordinate $(b\cos\theta, b\sin\theta, z)$, where b is the tube radius that is assumed to be of length $2L$. Similarly, with reference to the same rectangular Cartesian coordinate system (x, y, z), the center of the spherical TiO_2 has coordinates $(0, 0, Z)$, where Z is the distance between their centers, which can be either positive or negative. Thus, the distance ρ between the center of the TiO_2 and a typical point on the tube is given by

$$\rho^2 = b^2 + (z - Z)^2.$$

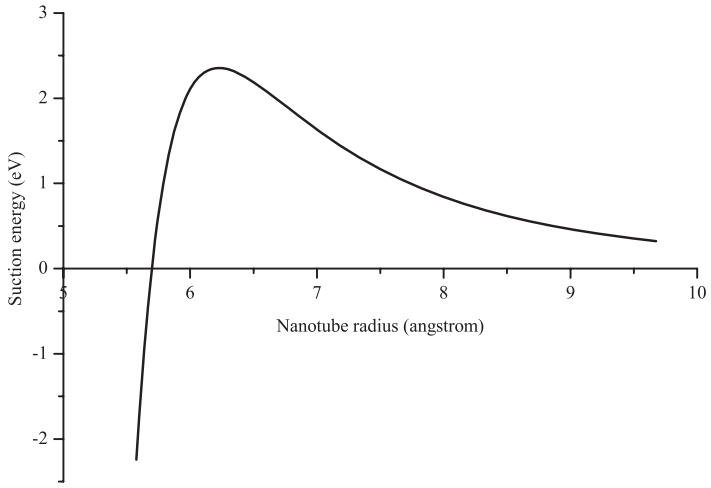

Figure 5. Suction energy for a cylindrical TiO_2 ($a = 2.6757$ Å).

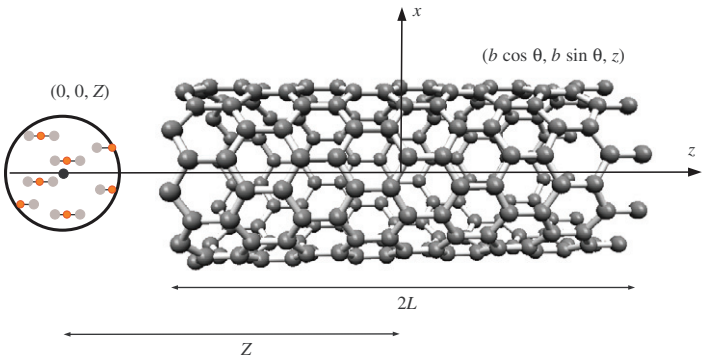

Figure 6. Spherical TiO_2 entering the CNT.

Utilizing the Lennard-Jones potential function and the continuum approximation, the total potential energy can be written as

$$U = \pi ab\eta_1\eta_2 \int_{-\pi}^{\pi}\int_{-L}^{L} \frac{1}{\rho}\left[\frac{A}{2}\left(\frac{1}{(\rho+a)^4} - \frac{1}{(\rho-a)^4}\right) - \frac{B}{5}\left(\frac{1}{(\rho+a)^{10}} - \frac{1}{(\rho-a)^{10}}\right)\right] \mathrm{d}z\,\mathrm{d}\theta,$$

and again, the force in the z-direction can be determined by the relation (2). Note that the consideration of the interaction energy and the force distribution for a spherical TiO_2 and a CNT is similar to that of a C_{60} fullerene inside a CNT [25].

To calculate the suction energy, we utilize the procedure for a C_{60} fullerene entering into a CNT as given by Cox *et al* [24]. Using the Lennard-Jones potential function together with the continuum approximation and assuming the CNT to be semi-infinite in length, the total potential energy can be written as

$$U = \pi ab\eta_1\eta_2 \int_{-\pi}^{\pi}\int_{0}^{\infty} \frac{1}{\rho}\left[\frac{A}{2}\left(\frac{1}{(\rho+a)^4} - \frac{1}{(\rho-a)^4}\right) - \frac{B}{5}\left(\frac{1}{(\rho+a)^{10}} - \frac{1}{(\rho-a)^{10}}\right)\right] \mathrm{d}z\,\mathrm{d}\theta. \quad (6)$$

Next we calculate the total potential energy via equation (5), but here we use (6) for the spherical case, and we use this result to calculate the suction energy. Figure 7 illustrates the

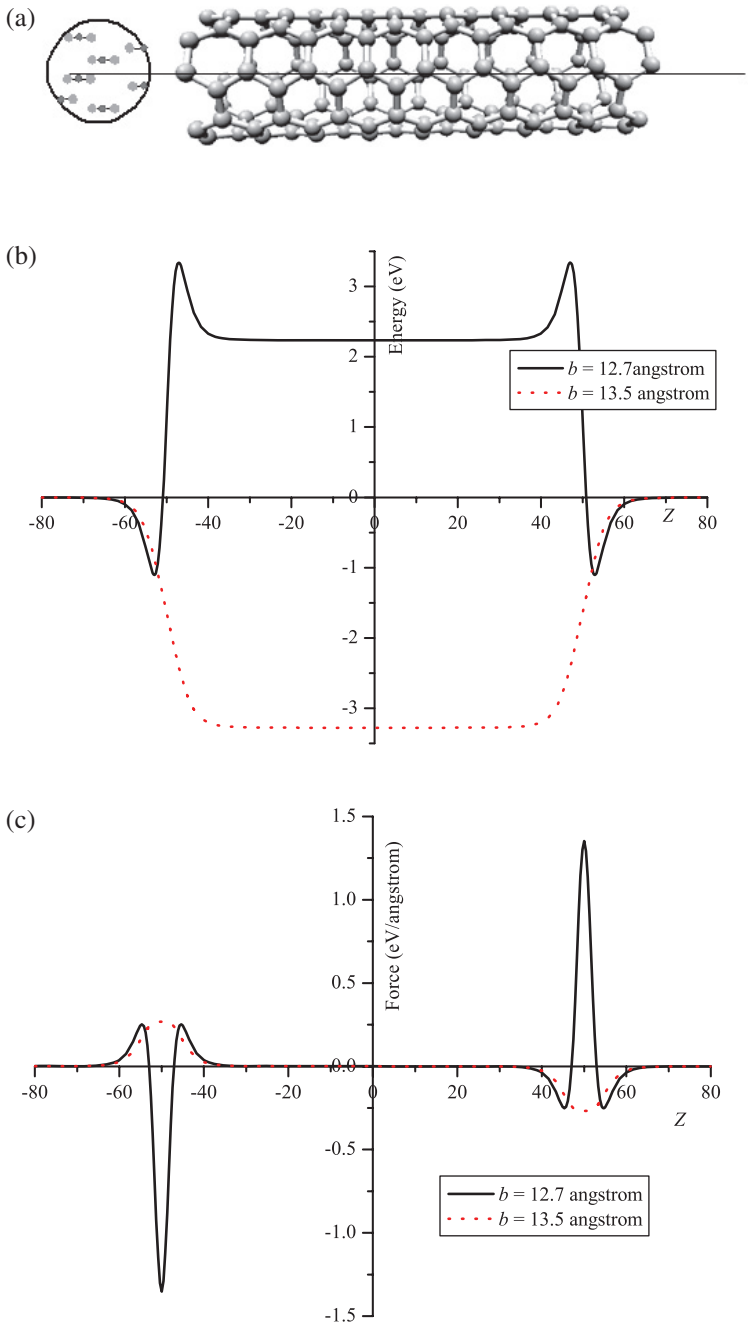

Figure 7. Spherical TiO_2 (a) with energy profile (b) and force distribution (c), where $a = 10$ Å, $b = 12.7$ and 13.5 Å and $L = 50$ Å.

interaction energy and the force distribution for the system. The radius of the spherical TiO_2 is assumed to be 10 Å, and the two radii of CNTs with length $L = 50$ Å are assumed to be 12.7 and 13.5 Å. Again we see that the TiO_2 molecule will enter into the CNT if the energy level inside the tube is lower than that outside of it. Once the TiO_2 molecule is encapsulated into the tube, it will not escape due to the barrier forces at tube's open ends.

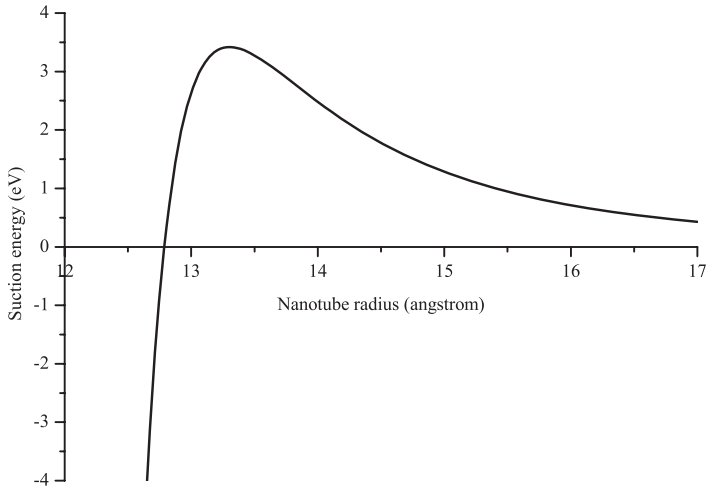

Figure 8. Suction energy for a spherical TiO_2 ($a = 10$ Å).

Assuming the radius of the spherical TiO_2 to be $a = 10$ Å, the suction profile for various CNTs is shown in figure 8. At $b = b_0 = 12.7954$ Å, the suction energy is zero, which agrees with the previous determination of the interaction energy and the force distribution. The maximum suction energy occurs when $b = 13.3042$ Å, consequently the radius differences is obtained as $b - a = 3.304$ Å. Again, the maximum suction energy is unvarying by changing the radii. Three TiO_2 radii, $a = 4$, 6 and 10 Å, are utilized to determine the suction energy, and we find that the maximum suction energy is linearly dependent on the TiO_2 radius, which is given by

$$\text{Maximum suction energy (eV)} = 0.41a(\text{Å}) - 0.69.$$

5. Concluding remarks

In this work, we have considered the mechanical characteristics for the encapsulation of TiO_2 nanoparticles into SWNTs. We employed the Lennard-Jones potential to calculate the van der Waals force, and we made the usual continuum approximation, for which the discrete carbon atoms are assumed to be replaced by an average distribution over each surface. The suction energy for TiO_2 entering an SWNT for the cases of cylindrical and spherical shape of titania was then determined. We find that the essential condition for the suction behavior depends on the difference of their radii ($b - a$). The advantage of our approach is that we are able to predict whether or not TiO_2 particles might be sucked into a CNT, which could become an important issue for applications involving drug delivery research.

In comparison to other methods used to study nanoscience and nanotechnology, such as first principle calculations, molecular dynamics or Monte Carlo simulations, our applied mathematical modeling approach is not been widely used in this field. The understanding obtained from our model could contribute to considerable insight into the basic concepts of the problem. To the authors' knowledge, no work has previously been undertaken using

mathematical modeling to describe the encapsulation behavior of TiO_2-NP into an SWNT. Our work thus could be viewed as a first experimental step toward designing new nanodevices, such as nanofluidic devices to control drug delivery, improve circulatory persistence, and allow the targeting of drugs to specific cells. It is commonly known that CNTs have the advantage of providing potential nanofluidic devices for controlling drug delivery which will help in the improvement of both circulatory persistence and the targeting of drugs to specific cells.

Acknowledgments

We thank David Blyler for editing the paper and our biophysics group members for reading the paper and providing helpful comments. We gratefully thank the Nanomechanics Group at the University of Wollongong, Australia. This work was partially supported by The Center of Excellence in Mathematics, The Center of Excellence for Innovation in Chemistry (PERCH-CIC), The Thailand Center of Excellence in Physics (ThEP), The Thailand Research Fund (TRF), The Mahidol University Research Grant, The Commission on Higher Education (CHE) and The Ministry of Education.

References

[1] Iijimaand S and Ichihashi T 1993 *Nature* **363** 603–5
[2] Bethune D S *et al* 1993 *Nature* **636** 605–7
[3] Calbi M M *et al* 2001 *Rev. Mod. Phys.* **73** 857–65
[4] Maniwa Y *et al* 2005 *Chem. Phys. Lett.* **401** 534–38
[5] Khlobystov A N *et al* 2004 *Phys. Rev. Lett.* **92** 245507
[6] Lee J *et al* 2002 *Nature* **415** 1005–8
[7] Smith B W, Monthioux M and Luzzi D E 1998 *Nature* **396** 323–4
[8] Okada S, Saito S and Oshiyama A 2001 *Phys. Rev. Lett.* **86** 3835–8
[9] Okada S, Otani M and Oshiyama A 2003 *Phys. Rev.* B **67** 205411
[10] Okada S 2005 *Phys. Rev.* B **72** 153409
[11] Linsebigler A L, Lu G and Yates J T 1995 *Chem. Rev.* **95** 735–58
[12] Chatterjee D and Dasgupta S 2005 *J. Photochem. Photobiol.* C **6** 186–205
[13] Wei C *et al* 1994 *Environ. Sci. Technol.* **28** 934–8
[14] Watts R J *et al* 1995 *Water Res.* **29** 95–100
[15] Lee S, Nakamura M and Ohgaki S 1998 *J. Environ. Sci. Health* A **33** 1643–55
[16] Sakai H *et al* 1994 *Biochem. Biophys. Acta* **1201** 259–65
[17] Blake D M *et al* 1999 *Sep. Purif. Methods* **28** 1–50
[18] Emeline A V, Frolov A B, Ryabchuk V K and Serpone N 2003 *J. Phys. Chem.* B **107** 7109–19
[19] Serpone N 1996 *The Kirk–Othmer Encyclopedia of Chemical Technology* (New York: Wiley)
[20] Srinivasan C and Somasundaram N 2003 *Curr. Sci.* **85** 1431–8
[21] Ireland J C, Klostermann P, Rice E W and Clark R 1993 *Appl. Environ. Microbiol.* **59** 1668–70
[22] Cho M, Chung H, Choi W and Yoon J 2005 *Appl. Environ. Microbiol.* **71** 270–5
[23] Lennard-Jones J E 1931 *Proc. Phys. Soc.* **43** 461–82
[24] Cox B J, Thamwattana N and Hill J H 2007 *Proc. R. Soc.* A **463** 461–76
[25] Cox B J, Thamwattana N and Hill J H 2007 *Proc. R. Soc.* A **463** 477–94
[26] Cox B J *et al* 2008 *Int. J. Nanotechnol.* **5** 195–217
[27] Hilder T A and Hill J H 2007 *J. Phys. A: Math. Theor.* **40** 3851–68

[28] Hilder T A and Hill J H 2007 *J. Appl. Phys.* **101** 064319
[29] Hilder T A and Hill J H 2007 *Phys. Rev.* B **75** 125415
[30] Baowan D, Thamwattana N and Hill J H 2008 *Commun. Nonlinear Sci. Numer. Simul.* **13** 1431–47
[31] Baowan D and Hill J M 2008 *J. Math. Chem.* **43** 1489–504
[32] Baowan D and Hill J M 2008 *J. Comput. Theor. Nanosci.* **5** 302–10
[33] Baowan D and Hill J M 2007 *Z Angew. Math. Phys.* **58** 857–75
[34] Fahmi A, Minot C, Silvi B and Causa M 1993 *Phys. Rev.* B **47** 11717–24
[35] Hirschfelder J O, Curtiss C F and Bird R B 1954 *Molecular Theory of Gases and Liquids* (New York: Wiley)
[36] Mayo S L, Olafson B D and Goddard W A III 1999 *J. Phys. Chem.* **94** 8897–909
[37] Girifalco L A, Hodak M and Lee R S 2000 *Phys. Rev.* B **62** 13104–10